Medicago truncatula copper transporter 1 (MtCOPT1) delivers copper for symbiotic nitrogen fixation

Marta Senovilla[1], Rosario Castro-Rodríguez[1], Isidro Abreu[1], Viviana Escudero[1], Igor Kryvoruchko[2,a], Michael K. Udvardi[2], Juan Imperial[2,3], Manuel González-Guerrero[1,b]

[1]Centro de Biotecnología y Genómica de Plantas (UPM-INIA). Campus de Montegancedo. Universidad Politécnica de Madrid. Crta. M-40 km 38. 28223 Pozuelo de Alarcón (Madrid). Spain.

[2]Plant Biology Division, The Samuel Roberts Noble Foundation, Ardmore, Oklahoma 73401.

[3]Consejo Superior de Investigaciones Científicas. Madrid. Spain.

[a]Present address: Bioengineering Department, Kafkas University, Kars 36100, Turkey.

[b]Corresponding author: Manuel González-Guerrero (manuel.gonzalez@upm.es). Phone: +34 91 3364558.

Total word count for the main text: 5439

Introduction word count: 1153

Materials and Methods word count: 1505

Results word count: 1237

Discussion word count: 1375

Acknowledgements word count: 86

Number of Figures: 8 (7 in colour)

Number of Supporting information files: 1 Table, 1 Supporting Materials and Methods, 1 Supporting Figure Legends, 8 Figures

Summary

- Copper is an essential nutrient for symbiotic nitrogen fixation. This element is delivered by the host plant to the nodule, where membrane copper transporter would introduce it into the cell to synthesize cupro-proteins.
- COPT family members in model legume *Medicago truncatula* were identified and their expression determined. Yeast complementation assays, confocal microscopy, and phenotypical characterization of a *Tnt1* insertional mutant line were carried out in the nodule-specific *M. truncatula* COPT family member.
- *Medicago truncatula* genome encodes eight COPT transporters. *MtCOPT1* (*Medtr4g019870*) is the only nodule-specific *COPT* gene. It is located in the plasma membrane of the differentiation, interzone and early fixation zones. Loss of MtCOPT1 function results in a copper-mitigated reduction of biomass production when the plant obtains its nitrogen exclusively from symbiotic nitrogen fixation. Mutation of *MtCOPT1* results in diminished nitrogenase activity in nodules, likely an indirect effect from the loss of a copper-dependent function, such as cytochrome oxidase activity in *copt1-1* bacteroids.
- These data are consistent with a model in which MtCOPT1 transports copper from the apoplast into nodule cells to provide copper for essential metabolic processes associated with symbiotic nitrogen fixation.

Keywords: symbiotic nitrogen fixation, copper transport, *Medicago truncatula*, nitrogenase, cytochrome oxidase.

Introduction

Symbiotic nitrogen fixation is the conversion of N_2 into NH_4^+ carried out by bacteria associated with host organisms, such as rhizobia inside legume root nodules (van Rhijn & Vanderleyden, 1995; Oldroyd, 2013; Downie, 2014). Legume root nodules result from a complex developmental program initiated by the exchange of chemical signals between the symbionts (Oldroyd, 2013; Antolín-Llovera et al., 2014). During this process, cells from the root cortex and from the endodermis and pericycle proliferate to form the nodule primordium (Xiao et al., 2014). In parallel, rhizobia are guided by infection threads from the root hairs to the inner cell layers of the nodule. There, in an endocytic-like process, they are released into the host cell cytosol, surrounded by a plant membrane called the symbiosome membrane (SM) (Limpens et al., 2009). The SM and enclosed rhizobia constitute a specialized, albeit transient, organelle called the symbiosome. Rhizobia within symbiosomes divide and eventually differentiate into nitrogen-fixing bacteroids as a microaerobic environment is established in the developing nodule (Vasse et al., 1990; Miller et al., 1993; Bobik et al., 2006). Two different nodule developmental programs are known: indeterminate, as in *Medicago* and *Pisum*; and determinate, as in *Lotus* and *Glycine*. The main difference is the persistence of a nodule meristem(s) in the indeterminate type, which gives rise to four contemporaneous developmental zones: the meristem (zone I); the infection/differentiation region where rhizobia are released from infection threads and differentiate into bacteroids (zone II) the nitrogen fixation zone (III); and the senescent zone (IV) (Vasse et al., 1990). In addition to this, some authors propose additional regions such as the interzone between Zone II and Zone III (Roux et al., 2014).

Transition metals, such as iron and copper, play an important role in symbiotic nitrogen fixation (Brear et al., 2013; González-Guerrero et al., 2014; González-Guerrero et al., 2016). Reduced levels of these metals in plants, caused by the low bioavailability of these nutrients in some soil types, have a detrimental effect on nitrogen fixation rates (Tang et al., 1992; Ibrikci & Moraghan, 1993; O'Hara, 2001). This results from their role as cofactors of many of the key enzymes involved symbiotic nitrogen fixation. Iron is part of the heme group that allows leghemoglobin to bind, transport, and buffer the nodule free O_2 at nanomolar levels and, thus, avoid nitrogenase poisoning (Appleby, 1984; Ott et al., 2005). Iron is also at the catalytical core of enzymes involved in free radical control (Hersleth et al., 2006) and in the metallic clusters in nitrogenase (Miller et al., 1993; Rubio

& Ludden, 2005). Copper is used in free radical metabolism in the nodule, as part of Cu,Zn superoxide dismutase (Rubio et al., 2004). It is also a cofactor of cytochrome oxidase, the final complex of an electron transport chain that reduces oxygen for energy metabolism. This system is essential for rhizobial survival, given their strictly aerobic metabolism. In fact, to survive in the microaerobic environment in the nodule and to satisfy the high-energy demands of symbiotic nitrogen fixation, a high-affinity copper-containing cytochrome *cbb*$_3$ oxidase is expressed by the bacteroids (Soupène et al., 1995; Preisig et al., 1996b; Udvardi & Poole, 2013). Loss of the activity of this enzyme results in loss of nitrogen fixation (Preisig et al., 1993), very likely as a consequence of the inability to provide sufficient energy to maintain nitrogenase activity at high enough levels, or of the increased oxygen levels that might result from missing this high-affinity O_2 reducing system.

Metallic micronutrients in rhizobia have to be provided by the host plant (Johnston et al., 2001). In the case of iron, and likely also for copper, they are carried by the vasculature from the root and released in the apoplast of the infection/differentiation zone in indeterminate type nodules, such as those of *Medicago truncatula* (Rodríguez-Haas et al., 2013). From there, a number of metal transporters introduce them in the cytosol of rhizobia-infected cells. In the case of iron, this is mediated by MtNramp1 (Tejada-Jiménez et al., 2015). In the case of copper, this could be mediated by a YSL (Yellow Stripe-Like) transporter if the substrate is nicotianamine-bound metal (Schaaf et al., 2004; Conte & Walker, 2011; Zheng et al., 2012), or by a COPT (Copper transporter) protein if it is Cu^+ (Sancenón et al., 2003; Pilon, 2011). Although nicotianamine seems to be important for SNF, as indicated by the loss of fixation capabilities in a mutant affected in the capability to synthesize this chelator (Avenhaus et al., 2016), the fact that iron is incorporated as Fe^{2+} (since it is mediated by a Nramp transporter) (Tejada-Jiménez et al., 2015) suggests that nicotianamine, and hence YSL proteins, is not be directly involved in metal uptake by rhizobia-infected cells.

COPT transporters, also known as Ctr in fungi and animals, are present in all eukaryotes (Lee et al., 2001; Zhou & Thiele, 2001; Sancenón et al., 2003). They are trimeric proteins in which the monomer is a 140-400 amino acid polypeptide with three transmembrane regions (Dumay et al., 2006). This protein has methionine-rich regions frequently present in the N-terminal extracytosolic region and a conserved MXXXM motif in the second transmembrane domain (De Feo et al., 2009). The later motif forms a

channel-like structure in the trimer that binds two Cu^{+} ions/trimer in a trigonal planar way (Dumay et al., 2006). In plants, COPT proteins constitute multigenic families (Sancenón et al., 2003; Yuan et al., 2011). Some of their members appear to be responsible for copper uptake from soil (Sancenon et al., 2004), in a manner very similar to that of iron uptake in Strategy I plants, *i.e.* transport of reduced metal produced by a ferroreductase-oxidase (FRO) protein, either FRO4 or FRO5 in *Arabidopsis thaliana* (Bernal et al., 2012). These transporters have also been associated with pollen development (Sancenon et al., 2004), remobilization of stored copper (Garcia-Molina et al., 2011), and copper allocation in aerial tissues (Garcia-Molina et al., 2013). However, in spite of the importance of copper in symbiotic nitrogen fixation (O'Hara, 2001; González-Guerrero et al., 2014; González-Guerrero et al., 2016), and the role of COPT proteins in copper uptake (Puig et al., 2007; Pilon, 2011), very little information is available about the role of these proteins in the nodule.

In this study, we have identified *MtCOPT1* (*Medtr4g019870*) a gene encoding a nodule-specific COPT family member. Consistent with a role in copper uptake from the apoplast, *MtCOPT1* expression is mainly confined to the differentiation/interzone region of the nodule, where its encoded protein is located in the plasma membrane of those cells. Characterization of a *Tnt1* insertional mutant in this gene showed a reduction in plant biomass production during symbiosis, associated with decreases in bacteroid cytochrome oxidase and nitrogenase activities. This was restored by transformation with a wild-type copy of the mutated gene or by increasing copper concentrations in the nutrient solution. This work adds to our understanding of how copper is delivered from the host plant to be used in symbiotic nitrogen fixation.

Materials and Methods

Biological materials and growth conditions

Medicago truncatula R108 seeds were scarified in concentrated H_2SO_4 for 7 min. Then, they were washed with cold water and surface-sterilized with 50% bleach for 90 s and incubated overnight in sterile water for imbibition. After 48 h at 4ºC, seeds were germinated in water-agar plates at 22ºC for 24 h. Then, seedlings were planted in sterile perlite pots and inoculated with *Sinorhizobium meliloti* 2011 or *S. meliloti* 2011 transformed with pHC60 (Cheng & Walker, 1998), as indicated. Plants were cultivated in a greenhouse in 16 h of light and 22ºC conditions, and watered every two days with

Jenner's solution or water, alternatively (Brito et al., 1994). Nodules were collected at 28 dpi. Non-nodulated plants were grown in similar conditions of light and temperature but instead of being inoculated with *S. meliloti,* they were watered every two weeks with solutions supplemented with 2 mM NH_4NO_3. For hairy-root transformations, *M. truncatula* seedlings were transformed with *Agrobacterium rhizogenes* ARqua1 carrying the appropriate binary vector as described (Boisson-Dernier et al., 2001). In agroinfiltration experiments, tobacco (*N. benthamiana*) leaves were transformed with the plasmid constructs in *A. tumefaciens* C58C1 (Deblaere et al., 1985). Tobacco plants were grown in a greenhouse under the same conditions as *M. truncatula*.

Saccharomyces cerevisiae strain *Δctr1* and its parental strain BY4741 (MATa *his3Δ 1 leu2Δ 0 met15Δ 0 ura3Δ0*) were purchased from the Yeast Knockout Collection (GE Dharmacon) and used for heterologous expression assays. Yeasts were grown in synthetic dextrose (SD), or in yeast peptone dextrose (YPD) media supplemented with 2 % glucose (Sherman et al., 1986). Phenotypic characterization was done in yeast peptone ethanol glycerol (YPEG) medium (Li & Kaplan, 2001).

Quantitative real-time RT-PCR

Transcriptional expression studies were carried out by real-time RT-PCR (StepOne plus, Applied Biosystems) using the Power SyBR Green master mix (Applied Biosystems). Primers used are indicated in Supplemental Table 1. RNA levels were normalized by using the *ubiquitin carboxy-terminal hydrolase* gene as internal standard for *M. truncatula* genes, and *pyruvate dehydrogenase B* for *S. meliloti* transcripts. RNA isolation and cDNA synthesis were carried out as previously described (Tejada-Jiménez et al., 2015).

Yeast complementation assays

MtCOPT1 cDNA was cloned between the *Xba*I and *Eco*RI sites of the expression vector pYPGE15. Restriction sites were added to *MtCOPT1* CDS by PCR, using the primers listed (Supporting Information, Table S1). Yeast were transformed using a lithium acetate-based method (Schiestl & Gietz, 1989). Transformants were selected in SD medium by uracil autotrophy. For phenotypic tests, transformants were plated in YPEG (Li & Kaplan, 2001) supplemented or not with 1 mM $CuSO_4$.

192

193 GUS staining

194 Two kb upstream of *MtCOPT1* start codon were amplified using the primers
195 indicated in Supporting Information, Table S1, then cloned in pDONR207 (Invitrogen)
196 and transferred to destination vector pGWB3 (Nakagawa et al., 2007) using Gateway
197 Cloning technology (Invitrogen). An *A. rhizogenes* ARqua1 derived strain transformed
198 with this pGWB3-based vector was used for hairy root transformation of *M. truncatula*
199 plants as indicated (Boisson-Dernier et al., 2001). Transformed plants were transferred to
200 sterilized perlite pots and inoculated with *S. meliloti* 2011. GUS activity was determined
201 in 28 dpi plants as described (Vernoud et al., 1999).

202

203 Immunohistochemistry and confocal microscopy

204 A DNA fragment integrating the full length *MtCOPT1* genomic region and the
205 two kb upstream of its start codon with three HA epitopes fused in N-terminus of the
206 protein, was cloned in the plasmid pGWB1 (Nakagawa et al., 2007) using Gateway
207 technology (Invitrogen). In frame fusion of the epitopes was done by fusion PCR using
208 the primers indicated in Supporting Information, Table S1. Hairy-root transformation was
209 performed as previously described (Boisson-Dernier et al., 2001). Transformed plants
210 were transferred to sterilized perlite pots and inoculated with *S. meliloti* 2011 containing
211 the pHC60 plasmid that constitutively expresses GFP. Nodules collected from 28-dpi
212 plants were fixed by overnight incubation in 4% paraformaldehyde, 2.5% sucrose in PBS
213 at 4ºC. After washing in PBS, nodules were cut in 100 µm sections with a Vibratome 1000
214 plus (Vibratome). Sections were dehydrated using methanol series (30, 50, 70, 100% in
215 PBS) for 5 min and then rehydrated. Cell walls were permeabilized with 4% cellulase in
216 PBS for 1 h at room temperature and with 0.1% Tween 20 in PBS for 15 min. Sections
217 were blocked with 5 % bovine serum albumin (BSA) in PBS before their incubation with
218 an anti-HA mouse monoclonal antibody (Sigma) for 2 hours at room temperature. After
219 washing, an Alexa594-conjugated anti-mouse rabbit monoclonal antibody (Sigma) was
220 added to the sections for 1 h at room temperature. DNA was stained with DAPI after
221 washing. Images were acquired with a confocal laser-scanning microscope (Leica SP8)
222 using excitation lights at 488 nm for GFP and at 561 nm for Alexa 594.

223

224 Transient *MtCOPT1* expression in Tobacco leaves

MtCOPT1 coding sequence was fused to GFP at N-terminus by cloning in pGWB6 (Nakagawa et al., 2007) using Gateway Technology (Invitrogen). These constructs, and the plasma membrane marker pm-CFP pBIN (Nelson et al., 2007) were introduced into *A. tumefaciens* C58C1 (Deblaere et al., 1985). Transformants were grown in liquid medium to late exponential phase. Then, cells were centrifuged and resuspended to an OD_{600} of 1.0 in 10 mM MES pH 5.6, containing 10 mM $MgCl_2$ and 150 µM acetosyringone. These cells were mixed with an equal volume of *A. tumefaciens* C58C1 expressing the silencing suppressor p19 of Tomato bushy stunt virus (pCH32 35S:p19) (Voinnet et al., 2003). Bacterial suspensions were incubated for 3 h at room temperature and then injected into young leaves of 4 week-old *Nicotiana benthamiana* plants. Leaves were examined after 3 days by confocal laser-scanning microscopy (Leica SP8) with excitation lights of 405 nm for CFP and 488 nm for GFP.

Acetylene reduction assay

Nitrogenase activity was measured by the acetylene reduction assay (Hardy et al., 1968). Nitrogen fixation was assayed in mutant and control plants at 28 dpi in 30 ml vials fitted with rubber stoppers. Each vial contained four or five pooled transformed plants. Three ml of air inside of the vial was replaced with 3 ml of acetylene. Tubes were incubated at room temperature for 30 min. Gas samples (0.5 ml) were analyzed in a Shimadzu GC-8A gas chromatograph fitted with a Porapak N column. The amount of ethylene produced was determined by measuring the height of the ethylene peak relative to background. Each point consists of two vials each. After measurements, nodules were recovered from roots to measure their weight.

Metal content determination

Total reflection X-ray fluorescence (TXRF) analysis was used to determine copper content in three sets of 28 dpi nodules, each set originating from the nodules pooled from five plants. Analyses were carried out at Total Reflection X-Ray Fluorescence laboratory from Interdepartmental Research Service (SIdI), Universidad Autónoma de Madrid (Spain). Inductively coupled plasma mass spectrometry (ICP-MS) was carried out in three sets of 28 dpi roots and shoots, each set originating from the nodules pooled from five plants. ICP-MS was carried out at the Unit of Metal Analysis from the Scientific and Technology Centre, Universidad de Barcelona (Spain).

258

259 Cytochrome oxidase activity

260 Nodules from 28-dpi plants were excised from the root and used for bacteroid
261 isolation, as described by Brito et al. (1994) with modifications. Final resuspension was
262 performed in 50 mM 4-(2-hydroxyethyl)-1-piperazineethanesulfonic acid (HEPES), 200
263 mM NaCl pH 7.0. Cytochrome oxidase activity was assessed using N,N,N',N'-
264 tetramethyl-p-phenylenediamine (TMPD) oxidation assay. The reaction was started by
265 adding TMPD to the bacteroid suspension to a final concentration of 2.7 mM. Each
266 sample was measured at OD_{520} each 10 s for 5 min to determine the reaction kinetics. To
267 measure protein content to calculate specific activity, the bacteroid suspension was lysed
268 in 10 % SDS at 90ºC for 5 min. Protein content was measured with the Pierce™ BCA
269 Protein Assay (Thermo Scientific), incubated for 30 minutes at 37 ºC and the absorbance
270 estimated at OD_{562}.

271

272 Bioinformatics

273 To identify *M. truncatula* COPT family members, BLASTN and BLASTX
274 searches were carried out in the *M. truncatula* Genome Project site
275 (http://www.jcvi.org/medicago/index.php). Sequences from model COPT proteins were
276 obtained from JCVI (http://www.jcvi.org/medicago/index.php), TAIR
277 (https://www.arabidopsis.org/), Rice Genome Annotation Project
278 (http://rice.plantbiology.msu.edu) and Uniprot (http://www.uniprot.org): *M. truncatula*
279 (MtCOPT1 to MtCOPT8: Medtr4g019870, Medtr7g066070, Medtr3g105330,
280 Medtr4g064963, Medtr4g065660, Medtr1g015000, Medtr4g065123, Medtr0027s0220),
281 *Arabidopsis thaliana* (AtCOPT1 to AtCOPT6: At5g59030, At3g46900, At5g59040,
282 At2g37925, At5g20650, At2g26975), *Oryza sativa* (OsCOPT1 to OsCOPT7:
283 Os01g56420, Os01g56430, Os03g25470, Os04g33900, Os05g35050, Os08g35490,
284 Os09g26900), *Brachypodium distachion* (BdCOPT1 to BdCOPT5: Bradi1g24180,
285 Bradi1g24190, Bradi2g51210, Bradi4g31330, Bradi5g09580), *Glycine max* (GmCOPT1
286 to GmCOPT9: Glyma_11g134700, Glyma_18g191300, Glyma_04g057000,
287 Glyma_06g057400, Glyma_01g106700, Glyma_07g141200, Glyma_07g141600,
288 Glyma_14g107100, Glyma_17g219400, Glyma_18g191900), *Phaseolus vulgaris*
289 (PvCOPT1 to PvCOPT6: Phavu_011g060400g, Phavu_011g060500g,
290 Phavu_008g112800g, Phavu_009g083400g, Phavu_008g113200g,

Phavu_009g083400g), *Solanum lycopersicum* (SlCOPT1 to SlCOPT8: Solyc02g082080, Solyc09g014870, Solyc06g005820, Solyc08g006250, Solyc10g084980, Solyc01g107640, Solyc09g011700, Solyc06g005620) and *Populus trichocarpa* (PtCOPT1 to PtCOPT9: Poptr_0009s04370g, Poptr_0001s25290g, Poptr_0009s04360g, Poptr_0006s09440g, Poptr_0006s23580g, Poptr_0006s14310g, Poptr_0006s09430g). Trees were constructed from a ClustalW multiple alignment of the sequences (http://www.ebi.ac.uk/Tools/msa/clustalw2), then analyzed by MEGA7 (Tamura *et al.,* 2013) using a Neighbour-Joining algorithm with bootstrapping (1,000 iterations). Unrooted trees were visualized with FigTree (http://tree.bio.ed.ac.uk/software/figtree).

Statistical tests

Data were analyzed with Student's unpaired t test to calculate statistical significance of observed differences. Test results with p-values lower than 0.05 were considered as statistically significant.

Results

MtCOPT1 is specifically expressed in nodules

The *M. truncatula* genome encodes eight *COPT* genes (*MtCOPT1, Medtr4g019870; MtCOPT2, Medtr7g066070; MtCOPT3, Medtr3g105330; MtCOPT4, Medtr4g064963; MtCOPT5, Medtr4g065660; MtCOPT6, Medtr1g015000; MtCOPT7, Medtr4g065123;* and *MtCOPT8, Medtr0027s0220*). Their expression profiles were determined in shoots, roots, and nodules in nodulated and non-nodulated plants. Out of the eight, *MtCOPT1* was the only gene whose transcripts were detected in nodules exclusively (Fig. 1a). *MtCOPT3* was the only other *COPT* gene also expressed in nodules, but it was not specific to this organ and its maximum expression occured in shoots, regardless of the symbiotic status of the plant (Supporting Information, Fig. S1). *MtCOPT4* and *MtCOPT6* transcripts were detected only in shoots of nodulated and non-nodulated plants, while *MtCOPT5* was mostly confined to roots. *MtCOPT8* transcripts were detected at low levels in both shoots and roots. No expression of *MtCOPT2* or *MtCOPT7* was observed in any of the samples assessed (Supporting Information, Fig. S1).

Sequence analyses of MtCOPT1 showed the conserved features of COPT1 proteins (Dumay et al., 2006; De Feo et al., 2009), with three predicted transmembrane

domains, and a conserved MXXXM domain in the second transmembrane region (Figure 1b). Sequence comparison of *M. truncatula* COPT transporters with those from other sequenced dicots and monocots revealed two major clusters of related sequences (Fig. 1c). MtCOPT1 is located in a branch shared by a subset of legume COPT proteins.

MtCOPT1 transports copper towards the cytosol

To confirm that MtCOPT1 was able to transport copper, yeast complementation assays were carried out using a *S. cerevisiae* mutant with a deletion in the *ScCTR1* gene. This mutant is affected in Cu^{+} uptake and, consequently, copper dependent metabolic reactions are affected. For instance, this strain is not able to grow on non-fermentable carbon sources since it lacks the copper-dependent cytochrome oxidase activity required. Therefore, this mutant was not able to grow on YPEG medium, that contains ethanol and glycerol as carbon sources (Li & Kaplan, 2001), unless the copper concentration of the medium was increased (Fig. 2). However, when these mutants were transformed with a vector expressing *MtCOPT1,* growth on YPEG under low copper conditions was restored to almost wild-type levels, indicating a role of MtCOPT1 in Cu^{+} uptake.

MtCOPT1 is a plasma membrane protein expressed in the nodule late differentiation, interzone, and early fixation zones

The different developmental zones of an indeterminate type nodule carry out different biological functions (Vasse et al., 1990). Consequently, as a first approach to discern the biological role of MtCOPT1, the expression profile in the nodule was determined by fusing the 2 kb region upstream of the start codon of *MtCOPT1* to a *β-glucuronidase* (*gus*) gene. Analysis of GUS activity in nodules of *A. rhizogenes*-transformed roots 28 days post inoculation (dpi) showed that expression was confined to the late infection/differentiation, interzone, and early fixation zone (Fig. 3a and b). Similar results were detected when using a *MtCOPT1*promoter::*green fluorescent protein* (*gfp*) fusion (Supporting Information, Fig. S2). This expression profile was very similar to the one recorded in the Symbimics database (https://iant.toulouse.inra.fr/symbimics/) that shows the transcripts in each nodule region (Fig. 3c) (Roux et al., 2014).

The above expression profile was also validated by detecting the protein localization using an epitope-labelled MtCOPT1 that has three hemagglutinin (HA) tags fused to its N-terminal region. Expression of this construct was driven by the same

promoter region as for the GUS activity visualization studies. MtCOPT1-HA was located in cells in the late infection/differentiation, interzone, and in the younger parts of the fixation zone (Fig. 4a). The protein was detected in both rhizobia-infected and non-infected cells. This result was not due to autofluorescence, since sections that were not incubated with the primary antibody did not show any signal (Supporting Information, Fig. S3). A closer view of these cells showed a peripheral distribution of the protein, indicative of a plasma-membrane localization (Fig. 4b). To validate this subcellular localization, *N. benthamiana* leaves where co-agroinfiltrated with a plasmid expressing a N-terminal GFP-labelled *MtCOPT1* under a 35S promoter and a plasma membrane marker fused to the cyan fluorescent protein (CFP). Confocal imaging of both constructs showed colocalization (Fig. 4c), validating the putative plasma membrane localization of MtCOPT1. No GFP signal was found in cells expressing the CFP-labelled PM marker alone, nor was CFP signal detected in cells containing only MtCOPT1-GFP (Supporting Information, Fig. S4), thus ruling out any non-specific signal when both constructs are co-expressed.

Loss of *MtCOPT1* function results in impaired, copper-mitigated nitrogenase activity

To determine the role of MtCOPT1 in *M. truncatula,* the *Transposable Element from N.tabacum* (*Tnt1*) mutant line NF19829 (*copt1-1*) was obtained from the Noble Foundation insertion mutant library (Tadege et al., 2008). This line carries a *Tnt1* insertion in position +32, that fully silences *MtCOPT1* expression (Fig. 5a). Mutating *MtCOPT1-1* had no significant effect on the expression levels of the other *M. truncatula COPT* family members (Supporting Information, Fig. S5)

Since *MtCOPT1* was expressed solely in nodules, the phenotype of *copt1-1* was assessed in *S. meliloti* inoculated plants watered with a nitrogen-deficient nutritive solution. Under these conditions, *copt1-1* showed reduced growth (Fig. 5b) and biomass (Fig. 5c) compared to wild-type plants. However, no significant differences were found in nodule number (Fig. 5d). Consistent with the role of MtCOPT1 in Cu^{+} transport in nodules, alterations in copper levels were detected in these organs, with over twice as much copper in *copt1-1* nodules than in wild-type ones (Fig. 5e). However, no major change in copper distribution was observed with copper sensor CS1 (Bernal et al., 2012; Chan et al., 2012) (Supporting Information, Fig. S6). Copper levels did not significantly differ between roots of wild-type or *copt1-1* plants, or between shoots of these two

genotypes. Acetylene reduction activity (Dilworth, 1966) was measured to determine how nitrogenase activity was affected by mutating *MtCOPT1*. The results showed a *ca.* 50% reduction of this activity in the *copt1-1* mutant (Fig. 5f). This phenotype can be attributed to the *Tnt1* insertion in *MtCOPT1* since it was restored by transforming *copt1-1* with *MtCOPT1* regulated by its own promoter (Fig. 5). To test whether the phenotype observed was caused by altered copper delivery to the plant, a plant nutrient solution fortified with a 100-fold excess of copper compared to our standard was used (Fig. 6). This resulted in improved growth of *copt1-1*, similar to that of wild type plants (Fig. 6a), and a restoration of biomass production (Fig. 6b) and of nitrogenase activity (Fig. 6c). No differences between wild-type and *copt1-1* plants were observed when they were not inoculated and an assimilable nitrogen source was provided in the nutrient solution (Supporting Information, Fig. S7).

Bacteroid cytochrome oxidase activity is impaired in *copt1-1* nodules

Although reduced nitrogenase activity could cause lower biomass production in *copt1-1* plants, there is no direct link between nitrogenase and copper nutrition. However, this enzymatic activity heavily relies on the obligatorily aerobic energy metabolism of the bacteroid, in which copper-dependent cytochrome oxidase cbb_3 plays a critical function. To test whether mutation in *MtCOPT1* had a negative impact on this metabolic process, cytochrome oxidase activity was measured in bacteroids isolated from *copt1-1* and wild-type nodules (Fig. 7). Bacteroids from *copt1-1* had 60 % less activity than the controls. Increasing copper concentration in the nutrient solution restored activity to levels similar to those of the wild type. This phenotype was not the result of down-regulation of the rhizobial cytochrome oxidase-encoding genes, since bacteroids from *copt1-1* had increased expression levels of their two *fixN* genes (Supporting Information, Fig. S8).

Discussion

Symbiotic nitrogen fixation heavily relies on a number of metalloproteins to carry out this complex and energetically costly reaction (Brear et al., 2013; González-Guerrero et al., 2014; González-Guerrero et al., 2016). Therefore, studying how metals are allocated from the host plant to the nitrogen-fixing rhizobia is of great importance in view of renewed efforts to engineer nitrogen fixation capabilities in non-legumes (Oldroyd & Dixon, 2014; Ivleva et al., 2016; Lopez-Torrejon et al., 2016; Mus et al., 2016). In this

423 context, a substantial effort has been dedicated to studying how iron is delivered to the
424 nodule and released into the apoplast (Rodríguez-Haas et al., 2013), a process likely
425 facilitated by citrate (Takanashi et al., 2013), to identify the plant transporters involved in
426 iron transport in rhizobia-infected cells (Kaiser et al., 2003; Hakoyama et al., 2012;
427 Tejada-Jiménez et al., 2015), and to describing mechanisms of iron buffering in the
428 bacteroid (Zielazinski et al., 2013). However, less is known about other transition metals
429 required for critical functions in symbiotic nitrogen fixation.

430 Copper is involved in several plant physiological processes: energy transduction
431 (cytochrome oxidase) (Brunori et al., 2005); cell wall metabolism (laccases) (Hakulinen
432 and Rouvinen, 2015); free radical metabolism (superoxide dismutase) (Fridovich, 1976);
433 hormone metabolism (ethylene receptor) (Rodríguez et al., 1999); and cofactor
434 biosynthesis (Cnx1) (Kuper et al., 2004). Copper deficiencies cause severe growth defects
435 in plants, associated with reduced photosynthetic rates and cell wall production
436 (Burkhead et al., 2009). It is also detrimental for symbiotic nitrogen fixation, a process
437 likely associated with reduced cytochrome oxidase activity in the bacteroids (O'Hara,
438 2001). Bacteroids carry out aerobic metabolism at extremely low free oxygen
439 concentrations in nodules, which requires the high-affinity cytochrome oxidase cbb_3 to
440 satisfy the energy demands of nitrogenase (Preisig et al., 1996b). This iron-copper
441 enzyme is assembled from the *fixNOQP* operon, but the copper cofactor is provided by a
442 subset of Cu^{+}-ATPases (FixI in rhizobia) that extrude this ion from the bacteroid cytosol
443 (Kahn et al., 1989; Preisig et al., 1996a; Raimunda et al., 2011; Patel et al., 2014). Both
444 *fixNOQP* and *fixGHIS* are expressed only in bacteroids, indicating roles in adaptation to
445 the endosymbiotic lifestyle. While we know how bacteroids transfer copper to this
446 cytochrome oxidase, less is known about how the metal is delivered by the host plant. In
447 analogy to how iron is delivered (Rodríguez-Haas et al., 2013; Tejada-Jiménez et al.,
448 2015), it might be hypothesized that it is carried out by the vasculature and released in
449 the apoplast of the infection/differentiation zone. Following this, a plasma membrane
450 copper transporter would introduce this element into the cell to be then delivered across
451 the symbiosome membrane to the bacteroids. Our results indicate that MtCOPT1 is
452 responsible for this apoplastic copper uptake.

453 *MtCOPT1* is a copper transporter expressed only in nodules. Yeast
454 complementation assays indicate that it is involved in copper uptake. *MtCOPT1*-
455 promoter::*gus/gfp* fusion studies indicate that this role is carried out in the region from

456 the late infection/differentiation zone to the early fixation zone, where it has been
457 suggested that copper would be released from the vasculature into the nodule apoplast
458 (Rodriguez-Haas et al., 2013). RNAseq data reported in the Symbimics database and
459 obtained from laser-captured microdissected cells in this region validate our expression
460 results (Roux et al., 2014). Moreover, the putative role of MtCOPT1 in introducing copper
461 into nodule cells is supported by the localization of HA-tagged MtCOPT1 in the
462 periphery, very likely the plasma membrane, of infected and non-infected cells. This was
463 confirmed by colocalization with a plasma membrane marker in tobacco leaves.

464 Normal plant growth under symbiotic conditions is dependent on MtCOPT1
465 activity, indicated by the reduced biomass production of *copt1-1* plants when compared
466 to the wild-type. This was the result of a *ca.* 50% reduction of nitrogenase activity, and
467 not to alterations in nodule development. This phenotype was caused by the *Tnt1* insertion
468 in *MtCOPT1* and not by any other insertion in a different part of the genome, since
469 transformation with *MtCOPT1* expressed under the control its own promoter was able to
470 restore wild-type growth and nitrogenase activity in *copt1-1*. However, MtCOPT1
471 transports Cu^{+}, and there is no evidence for a COPT/Ctr transporter with the ability to
472 transport iron or molybdenum, the two metal cofactors directly involved in nitrogenase
473 catalytic mechanism (Miller et al., 1993; Rubio and Ludden, 2005). Therefore, MtCOPT
474 must support nitrogen fixation indirectly, via a copper-dependent process. This idea is
475 supported by restoration of the wild-type phenotype after watering plants with a copper-
476 fortified nutrient solution.

477 One of the processes likely affected by alterations in copper homeostasis in the
478 nodule is cytochrome oxidase cbb_3 activity in the bacteroids. A malfunction in this
479 enzyme could result in a decrease in energy metabolism and/or an increase in free-oxygen
480 concentration, either of which could negatively affect nitrogenase activity. In fact, a
481 mutation in the *Bradyrhizobium japonicum fixNOQP* operon results in a fix^{-} phenotype
482 (Preisig et al., 1996b). A similar phenotype can be observed merely by mutating *fixI*, the
483 P_{1b}-ATPase that provides copper for this enzyme (Preisig et al., 1996a; Patel et al., 2014).
484 Bacteroids isolated from *copt1-1* nodules also showed a significant reduction in
485 cytochrome oxidase activity, consistent with a decrease in copper supply to bacteroids.
486 However, the *copt1-1* phenotype did not appear to be as severe as that of mutants in *fixI*
487 or in *fixN*, since some nitrogenase activity remained in the mutant nodules and no major
488 developmental change was observed. This indicates that MtCOPT1 is not the only

transporter responsible for copper uptake by these cells. The close homologue, MtCOPT2 is an unlikely candidate for this role, since its expression cannot be detected in nodules. On the other hand, MtCOPT3, the only other COPT family member expressed in nodules, could conceivably carry out this role. However, its expression is not affected by *MtCOPT1* mutation, which suggests that its role is independent of MtCOPT1, while its expression in every plant organ is indicative of a more general role in the plant physiology. Alternatively, another family of metal transporters, such as YSL, ZIP or Nramp, could carry out this role.

Our results also indicate the existence of a systemic metal deficiency signal originating in nodule cells. We detected a two-fold increase in copper levels in *copt1-1* mutant nodules compared to those of the wild type, which was somewhat of a surprise given the postulated role of MtCOPT1 in copper uptake by nodule cells. A possible explanation for this result is that cellular demand for copper in nodules is signalled systemically to increase supply to nodules until demand is met. In the absence of MtCOPT1 activity, intracellular levels of copper remain low, possibly triggering a systemic signal(s) that results in more copper being transported into nodules. Increased copper concentration in the apoplast appears to be sufficient to allow alternative transporters (e.g. COPTs, NRAMPs) to import some copper into cells, which would explain why some cytochrome oxidase activity was still detected in *copt1-1* nodules. However, the affinity for copper of alternative transporters must be relatively low, because very high concentrations of copper (100x) in the nutrient solution were required to complement the mutant phenotype. Similar observations have been made for the nodule-specific molybdate transporter *MtMOT1.3* (unpublished).

In conclusion, copper entering nodules is very likely delivered by the vasculature and released in the infection zone-interzone where MtCOPT1 would transport it into cells (Fig. 8). Within the cytoplasm, a Cu^{+}-chaperone (Robinson & Winge, 2010) would probably deliver the cation to other transporters and apo-proteins. In the case of the symbiosome, it could be hypothesized that a P_{1b}-ATPase mediates copper delivery to the bacteroid, since these ATPases have been shown to mediate copper transport (Burkhead et al., 2009; Kaplan & Lutsenko, 2009). However, no nodule-specific or nodule-induced Cu^{+}-ATPase has been reported to date either experimentally or from the available transcriptomic databases. Once in the symbiosome space, copper would be transported into the bacteroid, via transporters in both the outer and inner bacteroid membranes, and

522 subsequently delivered to cytochrome oxidase *cbb*$_3$ via FixI (Preisig et al., 1996a; Patel
523 et al., 2014; Trasnea et al., 2016; Fig. 8). This model does not exclude the existence of
524 other cuproproteins affected by *MtCOPT1* mutation, since once copper is within the
525 cytosol, it can be used in several different ways, and some of them could also potentially
526 affect nitrogenase activity in nodules.

527

528 **Acknowledgments**

529 This research was funded by the Spanish Ministry of Economy and
530 Competitiveness (grant number AGL-2012-32974) and by the European Research
531 Council Starting Grant (grant number ERC-2013-StG-335284) to MG-G. RC-R was
532 supported by a Formación del Personal Investigador fellowship (BES-2013-062674). Part
533 of the work was funded by the US National Science Foundation Plant Genome Research
534 Program (grant IOS1127155 to MU). The authors would like to thank Dr. Chris Chang
535 for providing the CS1 sensor, and Dr. José M. Argüello for sending us the DsRed-
536 expressing *S. meliloti.*

537

538 **Author contribution**

539 Phylogenetic tree, protein secondary structure prediction, yeast complementation,
540 and promoter:*gus* studies were carried out by M.S. Gene expression was determined by
541 M.S., and R.C.-R, as well as confocal microscopy studies. The *copt1-1* mutant was
542 obtained by I.K., and M.K.U. Phenotypic characterization of *copt1-1* was performed by
543 M.S., R.C.-R., I.A., and V.E. Bacteroid cytochrome oxidase activity was determined by
544 I.A., and M.S. J.I. and M.G.-G. were responsible for experimental design, data analyses,
545 and wrote the manuscript with contributions from all the authors.

546

FIGURE LEGENDS

Figure 1. *MtCOPT1* is a member of the COPT gene family and it is specifically expressed in nodules. (a) *MtCOPT1* expression in nodulated and non-nodulated plants. *M. truncatula ubiquitin carboxy-terminal hydrolase1* (MtUB1) expression was used as positive control for RT-PCR. (b) Proposed topology of MtCOPT1. The conserved MXXXM motif is marked with circles, with methionines indicated in green. (c) Unrooted tree of *M. truncatula* COPT transporters, and representative plant COPT homologues.

Figure 2. MtCOPT1 transports copper towards the cytosol. Yeast strain BY4741 was transformed with pYPGE15, while BY4741-derived Δ*ctr1* strain was transformed with either empty pYPGE15 or with pYPGE15 containing *MtCOPT1* coding sequence. Serial dilutions (10x) of each transformant were grown for 2 days at 28ºC in non-selective medium (YPD), in fermentative selective YPEG medium and in YPEG supplemented with 1 mM $CuSO_4$.

Figure 3. *MtCOPT1* gene is expressed in the infection, interzone and nitrogen fixation zones. (a) GUS staining of *M. truncatula* 28-dpi nodules expressing the *gus* gene under the control of *MtCOPT1* promoter. Bar = 300 µm. (b) Longitudinal section of a 28-dpi nodule expressing the *gus* gene under the control of *MtCOPT1* promoter. Bar = 100 µm. (c) Expression of *MtCOPT1* in *M. truncatula* nodules determined by laser-capture microdissection coupled to RNA sequencing. Data were obtained from the Symbimics database (https://iant.toulouse.inra.fr/symbimics/). Meris, meristem; Infec, infection one; Differ, differentiation zone; Inter, interzone; Fix, nitrogen fixation zone.

Figure 4. Subcellular localization of MtCOPT1-HA. (a) Cross section of a 28-dpi *M. truncatula* nodule inoculated with *S. meliloti* constitutively expressing GFP (green, upper right panel) and transformed with a vector expressing the fusion *MtCOPT1-HA* under the regulation of its endogenous promoter. Nodules were stained with DAPI to show DNA (blue, upper left panel). MtCOPT1-HA localization was determined using an Alexa 594-conjugated antibody (red, lower left panel). The lower right panel shows the overlay of the transillumination, DNA, *S. meliloti*, and MtCOPT1-HA. Scale bar =100 µm. (b) Detailed view of rhizobia-infected cells. GFP-expressing *S. meliloti* are shown in green, red indicates the position of MtCOPT1-HA, and blue is DAPI-stained DNA. Scale bar = 25 µm. (c) Localization of plasma membrane marker pm-CFP transiently expressed in tobacco leaf cells (left panel) and localization of MtCOPT1-GFP transiently expressed in

579 the same cells (central panel). Right panel shows the overlaid images and the
580 transillumination. Scale bar = 25 μm.

581 **Figure 5.** *MtCOPT1* mutation results in a reduced nitrogen fixation rate. (a) RT-PCR
582 amplification of *MtCOPT1* transcript in 28-dpi nodules of *M. truncatula* wild-type (WT)
583 and mutant (*copt1-1*) plants. *Ubiquitin carboxyl-terminal hydrolase1* (MtUb1) was used
584 as control for PCR amplifications. (b) Growth of representative plants of wild type, *copt1-*
585 *1*, and *copt1-1* transformed with a wild-type copy of *MtCOPT1*. Scale bar = 1 cm. (c)
586 Biomass production in shoots and roots. Data are the mean ± SD of at least 6
587 independently transformed plants. (d) Number of nodules per plant. Data are the mean ±
588 SD of at least 6 independently transformed plants. (e) Copper content in shoots, roots,
589 and nodules of wild type, *copt1-1*, and *copt1-1* transformed with *MtCOPT1*. Data are the
590 mean ± SD of three sets each with five independently transformed plants. (f) Nitrogenase
591 activity in 28-dpi nodules. Acetylene reduction was measured in duplicate in three sets,
592 each of four independently transformed plants. Data are the mean ± SD. Asterisk indicates
593 significant differences ($p<0.05$).

594 **Figure 6.** Copper complementation of the *copt1-1* phenotype. (a) Growth of
595 representative plants of wild type, and *copt1-1* watered with standard (16 μM Cu) or
596 copper fortified (1.6 mM Cu) nutrient solution. Scale bar = 3 cm. (b) Biomass production
597 in shoots and roots of wild type, and *copt1-1* watered with standard (16 μM Cu) or copper
598 fortified (1.6 mM Cu) nutrient solution. Data are the mean ± SD of at least 11 plants. (c)
599 Nitrogenase activity in 28-dpi nodules. Acetylene reduction was measured in duplicate in
600 three sets, each of four plants. Data are the mean ± SD. Asterisk indicates significant
601 differences ($p<0.05$).

602 **Figure 7.** Cytochrome oxidase activity in bacteroids isolated from wild-type and *copt1-*
603 *1* plants watered with standard (16 μM Cu) or copper fortified (1.6 mM Cu) nutrient
604 solution. Data are the mean ± SD of three sets of five pooled plants. Asterisk indicates
605 significant differences ($p<0.05$).

606 **Figure 8.** Model of copper homeostasis in rhizobia-infected nodule cells. Copper is
607 introduced into the host cell cytosol by MtCOPT1. There, Cu^+ will be transferred by
608 cytosolic Cu^+-chaperones to other cuproproteins or transported across the symbiosome
609 membrane, very likely by Cu^+-ATPases. Copper through some unknown transporters is
610 delivered into the bacteroid cytosol, where it will be bound by Cu^+-chaperone CopZ. This
611 protein will transfer copper to the Cu^+-ATPase FixI. In the periplasm, copper will be

612 delivered to SenC, which will add the copper cofactor to cytochrome oxidase *cbb*$_3$. In
613 addition to MtCOPT1, other copper uptake systems must exist. Candidates are MtCOPT3,
614 the other COPT family member expressed in nodules, or a member of the Nramp, ZIP, or
615 YSL metal transport families. PM stands for plasma membrane, SM for symbiosome
616 membrane, OM for bacteroid outer membrane, and IM for bacteroid inner membrane.
617
618
619
620
621
622
623
624
625
626
627
628
629
630
631
632
633
634
635
636
637
638
639
640
641

642 **References**

643 **Antolín-Llovera M, Petutsching EK, Ried MK, Lipka V, Nürnberger T, Robatzek**
644 **S, Parniske M. 2014**. Knowing your friends and foes - plant receptor-like kinases as
645 initiators of symbiosis or defence. *New Phytologist* **204**: 791-802.
646 **Appleby CA 1984**. Leghemoglobin and *Rhizobium* respiration. *Annual Review of Plant*
647 *Physiology* **35**: 443-478.
648 **Avenhaus U, Cabeza RA, Liese R, Lingner A, Dittert K, Salinas-Riester G,**
649 **Pommerenke C, Schulze J. 2016**. Short-term molecular acclimation processes of legume
650 nodules to increased external oxygen concentration. *Frontiers in Plant Science* **6**: 1012.
651 **Bernal M, Casero D, Singh V, Wilson GT, Grande A, Yang H, Dodani SC, Pellegrini**
652 **M, Huijser P, Connolly EL, et al. 2012**. Transcriptome sequencing identifies SPL7-
653 regulated copper acquisition genes *FRO4/FRO5* and the copper dependence of iron
654 homeostasis in *Arabidopsis*. *Plant Cell* **24**: 738-761.
655 **Bobik C, Meilhoc E, Batut J. 2006**. FixJ: a major regulator of the oxygen limitation
656 response and late symbiotic functions of *Sinorhizobium meliloti*. *Journal of Bacteriology*
657 **188**: 4890-4902.
658 **Boisson-Dernier A, Chabaud M, Garcia F, Bécard G, Rosenberg C, Barker DG.**
659 **2001**. *Agrobacterium rhizogenes*-transformed roots of *Medicago truncatula* for the study
660 of nitrogen-fixing and endomycorrhizal symbiotic associations. *Molecular Plant-*
661 *Microbe Interactions* **14**: 695-700.
662 **Brear EM, Day DA, Smith PMC. 2013**. Iron: an essential micronutrient for the legume–
663 rhizobium symbiosis. *Frontiers in Plant Science* **4**: 359.
664 **Brito B, Palacios JM, Hidalgo E, Imperial J, Ruíz-Argüeso T. 1994**. Nickel
665 availability to pea (*Pisum sativum* L.) plants limits hydrogenase activity of *Rhizobium*
666 *leguminosarum* bv. *viciae* bacteroids by affecting the processing of the hydrogenase
667 structural subunits. *Journal of Bacteriology* **176**: 5297-5303.
668 **Brunori M, Giuffre A, Sarti P. 2005**. Cytochrome c oxidase, ligands and electrons.
669 *Journal of Inorganic Biochemistry* **99**: 324-336.
670 **Burkhead JL, Gogolin Reynolds KA, Abdel-Ghany SE, Cohu CM, Pilon M. 2009**.
671 Copper homeostasis. *New Phytologist* **182,** 799-816.
672 **Chan J, Dodani SC, Chang CJ. 2012**. Reaction-based small-molecule fluorescent
673 probes for chemoselective bioimaging. *Nature Chemistry* **4**; 973-984.

674 **Cheng HP, Walker GC. 1998**. Succinoglycan is required for initiation and elongation of
675 infection threads during nodulation of alfalfa by *Rhizobium meliloti*. *Journal of*
676 *Bacteriology* **180**: 5183-5191.
677 **Conte S, Walker EL. 2011**. Transporters contributing to iron trafficking in plants.
678 *Molecular Plant* **4**: 464-476.
679 **De Feo CJ, Aller SG, Siluvai GS, Blackburn NJ, Unger VM. 2009**. Three-dimensional
680 structure of the human copper transporter hCTR1. *Proceedings of the National Academy*
681 *of Sciences, USA* **106**: 4237-4242.
682 **Deblaere R, Bytebier B, de Greve H, Deboeck F, Schell J, van Montagu M, Leemans**
683 **J. 1985**. Efficient octopine Ti plasmid-derived vectors for *Agrobacterium*-mediated gene
684 transfer to plants. *Nucleic Acids Research* **113**: 4777-4788.
685 **Dilworth MJ. 1966**. Acetylene reduction by nitrogen-fixing preparations from
686 *Clostridium pasteurianum*. *Biochimicia et Biophysica Acta* **127**: 69-90.
687 **Downie JA. 2014**. Legume nodulation. *Current Biology* **24**: R184-R190.
688 **Dumay QC, Debut AJ, Mansour NM, Saier MH. 2006**. The copper transporter (Ctr)
689 family of Cu^{+} uptake systems. *Journal of Molecular Microbiology and Biotechnology* **11**:
690 10-19.
691 **Fridovich I. 1976**. Superoxide dismutases: studies of structure and mechanism. *Advances*
692 *in Experimental Medicine and Biology* **74**: 530.539.
693 **Garcia-Molina A, Andrés-Colás N, Perea-García A, del Valle-Tascón S, Peñarrubia**
694 **L, Puig S. 2011**. The intracellular Arabidopsis COPT5 transport protein is required for
695 photosynthetic electron transport under severe copper deficiency. *Plant Journal* **65**: 848-
696 860.
697 **Garcia-Molina A, Andrés-Colás N, Perea-García A, Neumann U, Dodani SC,**
698 **Huijser P, Peñarrubia L, Puig S. 2013**. The *Arabidopsis* COPT6 transport protein
699 functions in copper distribution under copper-deficient conditions. *Plant and Cell*
700 *Physiology* **54**: 1378-1390.
701 **González-Guerrero M, Matthiadis A, Sáez Á, Long TA. 2014**. Fixating on metals: new
702 insights into the role of metals in nodulation and symbiotic nitrogen fixation. *Frontiers*
703 *in Plant Science* **5**: 45.
704 **González-Guerrero M, Escudero V, Sáez Á, Tejada-Jiménez M. 2016**. Transition
705 metal transport in plants and associated endosymbionts. Arbuscular mycorrhizal fungi
706 and rhizobia. *Frontiers in Plant Science* **7**: 1088.

Hakoyama T, Niimi K, Yamamoto T, Isobe S, Sato S, Nakamura Y, Tabata S, Kumagai H, Umehara Y, Brossuleit K, et al. 2012. The integral membrane protein SEN1 is required for symbiotic nitrogen fixation in *Lotus japonicum* nodules. *Plant and Cell Physiology* **53,** 225-236.

Hakulinen N, Rouvinen J. 2015. Three-dimensional structures of laccases. *Cellular and Molecular Life Sciences* **72**: 857-868.

Hardy RW, Holsten RD, Jackson EK, Burns RC. 1968. The acetylene-ethylene assay for n(2) fixation: laboratory and field evaluation. *Plant Physiology* **43**: 1185-1207.

Hersleth HP, Ryde U, Rydberg P, Görbitz CH, Andersson KK. 2006. Structures of the high-valent metal-ion haem-oxygen intermediates in peroxidases, oxygenases and catalases. *Journal of Inorganic Biochemistry* **100**: 460-476.

Ibrikci H, Moraghan JT. 1993. Differential responses of soybean and dry bean to zinc deficiency. *Journal of Plant Nutrition* **16**: 1791-1805.

Ivleva NB, Groat J, Staub JM, Stephens M. 2016. Expression of active subunit of nitrogenase via integration into plant organelle genome. *PLoS One* **11**: e0160951.

Johnston AW, Yeoman KH, Wexler M. 2001. Metals and the rhizobial-legume symbiosis - uptake, utilization and signalling. *Advances in Microbial Physiology* **45**: 113-156.

Kahn D, David M, Domergue O, Daveran ML, Ghai J, Hirsch PR, Batut J. 1989. *Rhizobium meliloti fixGHI* sequence predicts involvement of a specific cation pump in symbiotic nitrogen fixation. *Journal of Bacteriology*. **171**: 929-939.

Kaiser BN, Moreau S, Castelli J, Thomson R, Lambert A, Bogliolo S, Puppo A, Day DA. 2003. The soybean NRAMP homologue, GmDMT1, is a symbiotic divalent metal transporter capable of ferrous iron transport. *Plant Journal* **35**: 295-304.

Kaplan JH, Lutsenko S. 2009. Copper transport in mammalian cells: Special care for a metal with special needs. *Journal of Biological Chemistry* **284**: 25461-25465.

Kobayashi T, Nishizawa NK. 2012. Iron uptake, translocation, and regulation in higher plants. *Annual Review of Plant Biology* **63**: 131-152.

Kuper J, Llamas A, Hecht HJ, Mendel RR, Schwarz G. 2004. Structure of the molybdopterin-bound Cna1G domain links molybdenum and copper metabolism. *Nature* **430**: 803-806.

Lee J, Prohaska JR, Thiele DJ. 2001. Essential role for mammalian copper transporter Ctr1 in copper homeostasis and embryonic development. *Proceedings of the National Academy of Sciences, USA* **98**: 6842-6847.

741 **Li L, Kaplan J. 2001**. The yeast gene *MSC2*, a member of the cation diffusion facilitator
742 family, affects the cellular distribution of zinc. *Journal of Biological Chemistry* **276**:
743 5036-5043.
744 **Limpens E, Ivanov S, van Esse W, Voets G, Fedorova E, Bisseling T. 2009**. *Medicago*
745 N_2-fixing symbiosomes acquire the endocytic identity marker Rab7 but delay the
746 acquisition of vacuolar identity. *Plant Cell* **21**: 2811-2828.
747 **Lopez-Torrejon G, Jimenez-Vicente E, Buesa JM, Hernandez JA, Verma HK,**
748 **Rubio LM. 2016**. Expression of a functional oxygen-labile nitrogenase component in the
749 mitochondrial matrix of aerobically grown yeast. *Nature Communications* **7,** 11426.
750 **Miller RW, Yu Z, Zarkadas CG. 1993**. The nitrogenase proteins of *Rhizobium meliloti*:
751 purification and properties of the MoFe and Fe components. *Biochimica et Biophysica*
752 *Acta* **1163,** 31-41.
753 **Mus F, Crook MB, Garcia K, Garcia Costas A, Geddes BA, Kouri ED, Paramasivan**
754 **P, Ryu MH, Oldroyd GE, Poole PS, et al. 2016**. Symbiotic nitrogen fixation and
755 challenges to extending it to non-legumes. *Applied and Environmental Microbiology* **82,**
756 3698-3710.
757 **Nakagawa T, Kurose T, Hino T, Tanaka K, Kawamukai M, Niwa Y, Toyooka K,**
758 **Matsuoka K, Jinbo T, Kimura, T. 2007**. Development of series of gateway binary
759 vectors, pGWBs, for realizing efficient construction of fusion genes for plant
760 transformation. *Journal of Bioscience and Bioengineering* **104**: 34-41.
761 **Nelson BK, Cai X, Nebenführ A. 2007**. A multi-color set of in vivo organelle markers
762 for colocalization studies in *Arabidopsis* and other plants. *Plant Journal* **51**: 1126-1136.
763 **O'Hara GW. 2001**. Nutritional constraints on root nodule bacteria affecting symbiotic
764 nitrogen fixation: a review. *Australian Journal of Experimental Agriculture* **41**: 417-433.
765 **Oldroyd GE, Dixon R. 2014**. Biotechnological solutions to the nitrogen problem.
766 *Current Opinion in Biotechnology* **26**: 19-24.
767 **Oldroyd GE. 2013**. Speak, friend, and enter: signalling systems that promote beneficial
768 symbiotic associations in plants. *Nature Reviews Microbiology* **11**: 252-263.
769 **Ott T, van Dongen JT, Guther C, Krusell L, Desbrosses G, Vigeolas H, Bock V,**
770 **Czechowski T, Geigenberger P, Udvardi MK. 2005.** Symbiotic leghemoglobins are
771 crucial for nitrogen fixation in legume root nodules but not for general plant growth and
772 development. *Current Biology* **15**: 531-5.

773 **Patel SJ, Padilla-Benavides T, Collins JM, Argüello JM. 2014**. Functional diversity of
774 five homologous Cu^{+}-ATPases present in *Sinorhizobium meliloti*. *Microbiology* **160**:
775 1237-1251.
776 **Pilon, M.** (2011). Moving copper in plants. *New Phytologist* **192**: 305-307.
777 **Preisig O, Anthamatten D, Henneck H. 1993**. Genes for a microaerobically induced
778 oxidase complex in *Bradyrhizobium japonicum* are essential for a nitrogen-fixing
779 endosymbiosis. *Proceedings of the National Academy of Sciences, USA* **90**: 3309-3313.
780 **Preisig O, Zufferey R, Hennecke H. 1996a**. The *Bradyrhizobium japonicum fixGHIS*
781 genes are required for the formation of the high-affinity cbb(3)-type cytochrome oxidase.
782 *Archives of Microbiology* **165**: 297-305.
783 **Preisig O, Zufferey R, Thony-Meyer L, Appleby C, Hennecke H. 1996b**. A high-
784 affinity cbb3-type cytochrome oxidase terminates the symbiosis- specific respiratory
785 chain of *Bradyrhizobium japonicum*. *Journal of Bacteriology* **178**: 1532-1538.
786 **Puig S, Andés-Colás N, García-Molina A, Peñarrubia, L. 2007**. Copper and iron
787 homeostasis in Arabidopsis: responses to metal deficiencies, interactions and
788 biotechnological applications. *Plant, Cell & Environment* **30**: 271-290.
789 **Raimunda D, González-Guerrero M, Leeber BW, Argüello JM. 2011**. The transport
790 mechanism of bacterial Cu(+)-ATPases: distinct efflux rates adaptated to different
791 function. *Biometals* **24,** 467-475.
792 **Robinson NJ, Winge DR. 2010**. Copper metallochaperones. *Annual Review in*
793 *Biochemistry* **79**: 537-562.
794 **Rodríguez FI, Esch JJ, Hall AE, Binder BM, Schaller GE, Bleecker AB. 1999**. A
795 copper cofactor for the ethylene receptor ETR1 from *Arabidopsis*. *Science* **283**: 996.
796 **Rodríguez-Haas B, Finney L, Vogt S, González-Melendi P, Imperial J, González-**
797 **Guerrero M. 2013**. Iron distribution through the developmental stages of *Medicago*
798 *truncatula* nodules. *Metallomics* **5,** 1247-1253.
799 **Roux B, Rodde N, Jardinaud MF, Timmers T, Sauviac L, Cottret L, Carrère S,**
800 **Sallet E, Courcelle E, Moreau S, et al. 2014**. An integrated analysis of plant and
801 bacterial gene expression in symbiotic root nodules using laser-capture microdissection
802 coupled to RNA sequencing. *Plant Journal* **77,** 817-837.
803 **Rubio LM, Ludden PW. 2005**. Maturation of nitrogenase: a biochemical puzzle. *Jornal*
804 *of Bacteriology* **187**: 405-414.

Rubio MC, James EK, Clemente MR, Bucciarelli B, Fedorova M, Vance CP, Becana M. 2004. Localization of superoxide dismutases and hydrogen peroxide in legume root nodules. *Molecular Plant-Microbe Interactions* **17**: 1294-1305.

Sancenon V, Puig S, Mateu-Andres I, Dorcey E, Thiele DJ, Penarrubia L. 2004. The arabidopsis copper transporter COPT1 functions in root elongation and pollen development. *Journal of Biological Chemistry* **279**: 15348-15355.

Sancenón V, Puig S, Mira H, Thiele D, Peñarrubia L. 2003. Identification of a copper transporter family in *Arabidopsis thaliana*. *Plant Molecular Biology* **51**: 577-587.

Schaaf G, Ludewig U, Erenoglu BE, Mori S, Kitahara T, von Wiren N. 2004. ZmYS1 functions as a proton-coupled symporter for phytosiderophore- and nicotianamine-chelated metals. *Journal of Biological Chemistry* **279**: 9091-9096.

Schiestl RH, Gietz RD. 1989. High efficiency transformation of intact yeast cells using single stranded nucleid acids as a carrier. *Current Genetics* **16**: 339-346.

Sherman F, Fink GR, Hicks JB. 1986. *Methods in yeast genetics*. Plainview, NY: Cold Spring Harbor Lab Press.

Soupène E, Foussard M, Boistard P, Truchet G, Batut J. 1995. Oxygen as a key developmental regulator of *Rhizobium meliloti* N_2-fixation gene expression within the alfalfa root nodule. *Proceedings of the National Academy of Sciences, USA* **92**: 3759-3763.

Tadege M, Wen J, He J, Tu H, Kwak Y, Eschstruth A, Cayrel A, Endre G, Zhao PX, Chabaud M, et al. 2008. Large-scale insertional mutagenesis using the Tnt1 retrotransposon in the model legume *Medicago truncatula*. *Plant Journal* **54**: 335-347.

Takanashi K, Yokosho K, Saeki K, Sugiyama A, Sato S, Tabata S, Ma JF, Yazaki K. 2013. LjMATE1: a citrate transporter responsible for iron supply to the nodule infection zone of *Lotus japonicus*. *Plant and Cell Physiology* **54**: 585-594.

Tang CX, Robson AD, Dilworth MJ, Kuo J. 1992. Microscopic evidence on how iron-deficiency limits nodule initiation in *Lupinus angustifolius* l. *New Phytologist* **121**: 457-467.

Tejada-Jiménez M, Castro-Rodríguez R, Kryvoruchko I, Lucas MM, Udvardi M, Imperial J, González-Guerrero M. 2015. *Medicago truncatula* Natural Resistance-Associated Macrophage Protein1 is required for iron uptake by rhizobia-infected nodule cells. *Plant Physiology* **168,** 258-272.

Trasnea PI, Utz M, Khalfaoui-Hassani B, Lagies S, Daldal F, Koch HG. 2016. Cooperation between two periplasmic copper chaperones is required for full activity of

839 the cbb3-type cytochrome c oxidase and copper homeostasis in *Rhodobacter capsulatus*.
840 *Molecular Microbiology* **100**: 345-361.
841 **Udvardi M, Poole PS. 2013**. Transport and metabolism in legume-rhizobia symbioses.
842 *Annual Review of Plant Biology* **64**: 781-805.
843 **van Rhijn P, Vanderleyden J. 1995**. The Rhizobium-plant symbiosis. *Microbiological*
844 *Reviews* **59**: 124-142.
845 **Vasse J, de Billy F, Camut S, Truchet G. 1990**. Correlation between ultrastructural
846 differentiation of bacteroids and nitrogen fixation in alfalfa nodules. *Journal of*
847 *Bacteriology* **172**: 4295-4306.
848 **Vernoud V, Journet EP, Barker DG. 1999**. *MtENOD20*, a Nod factor-inducible
849 molecular marker for root cortical cell activation. *Molecular Plant-Microbe Interactions*
850 **12**: 604-614.
851 **Voinnet O, Rivas S, Mestre P, Baucombe D. 2003**. An enhanced transient expression
852 system in plants based on suppression of gene silencing by the p19 protein of tomato
853 bushy stunt virus. Plant Journal **33,** 949-956.
854 **Xiao TT, Schilderink S, Moling S, Deinum EE, Kondorosi E, Franssen H, Kulikova**
855 **O, Niebel A, Bisseling T. 2014**. Fate map of *Medicago truncatula* root nodules.
856 *Development* **141**: 3517-3528.
857 **Yuan M, Li X, Xiao J, Wang S. 2011**. Molecular and functional analyses of COPT/Ctr-
858 type copper transporter-like gene family in rice. *BMC Plant Biology* **11**: 69.
859 **Zheng L, Yamaji N, Yokosho K, Ma JF. 2012**. YSL16 Is a phloem-localized transporter
860 of the copper-nicotianamine complex that is responsible for copper distribution in rice.
861 *Plant Cell* **24**: 3767-3782.
862 **Zhou H, Thiele DJ. 2001**. Identification of a novel high affinity copper transport
863 complex in the fission yeast *Schizosaccharomyces pombe*. *Journal of Biological*
864 *Chemistry* **276**: 20529-20535.
865 **Zielazinski EL, González-Guerrero M, Subramanian P, Stemmler TL, Argüello JM,**
866 **Rosenzweig AC. 2013**. *Sinorhizobium meliloti* Nia is a P1B-5-ATPase expressed in the
867 nodule during plant symbiosis and is involved in Ni and Fe transport. *Metallomics* **5,**
868 1614-1623.

869

FIGURE 1

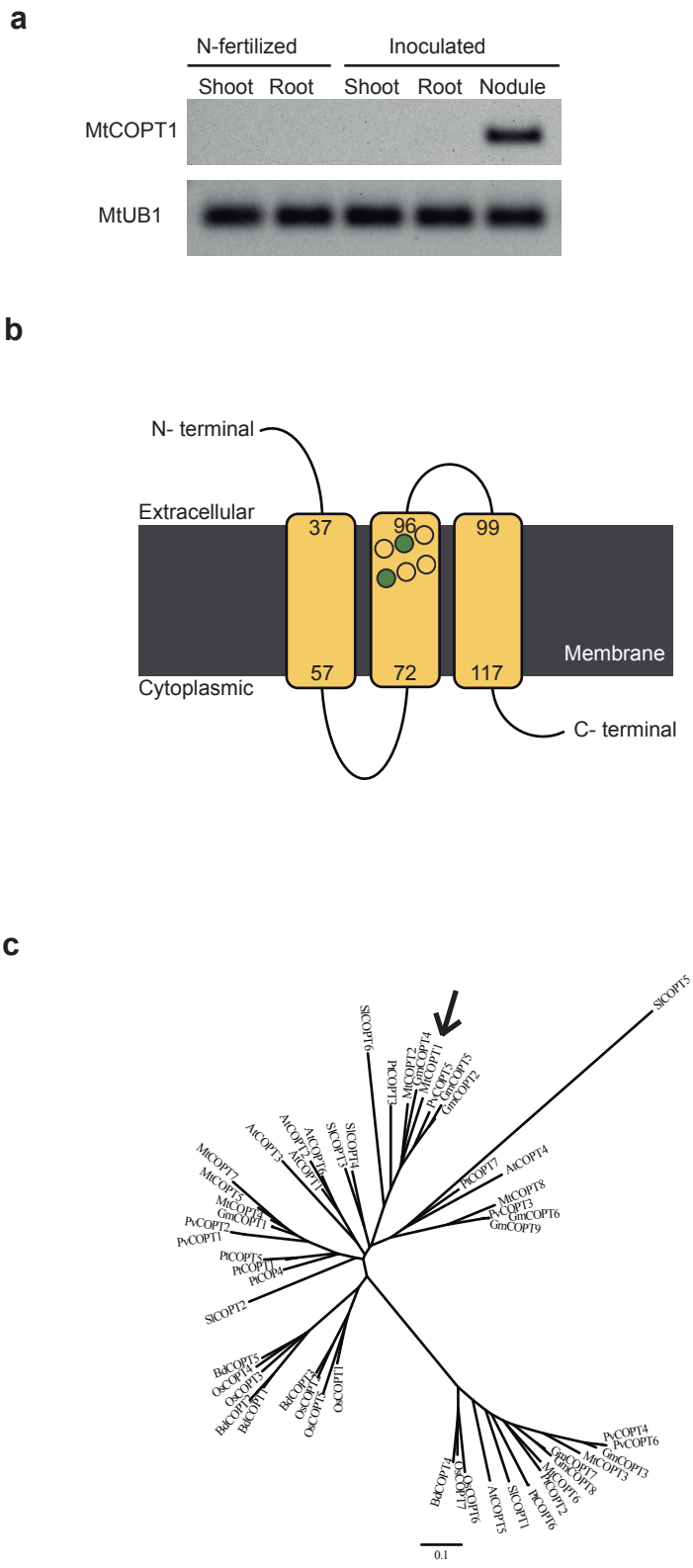

FIGURE 2

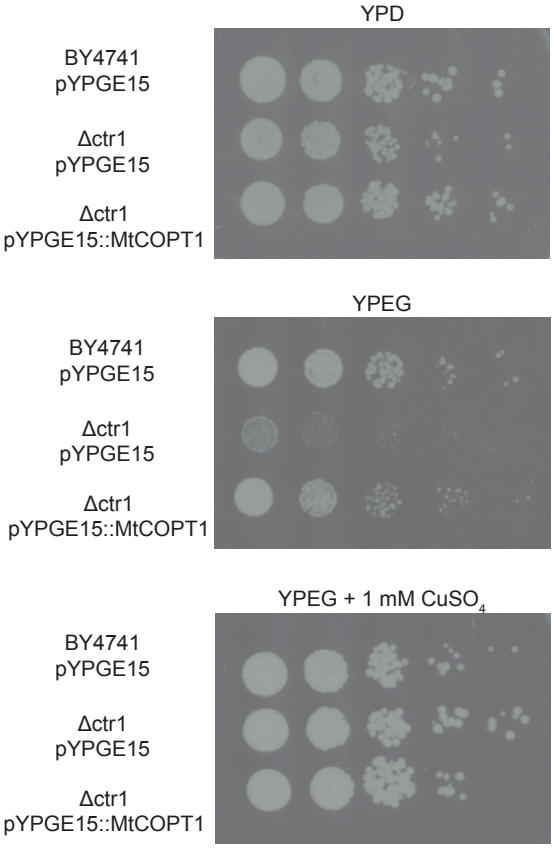

FIGURE 3

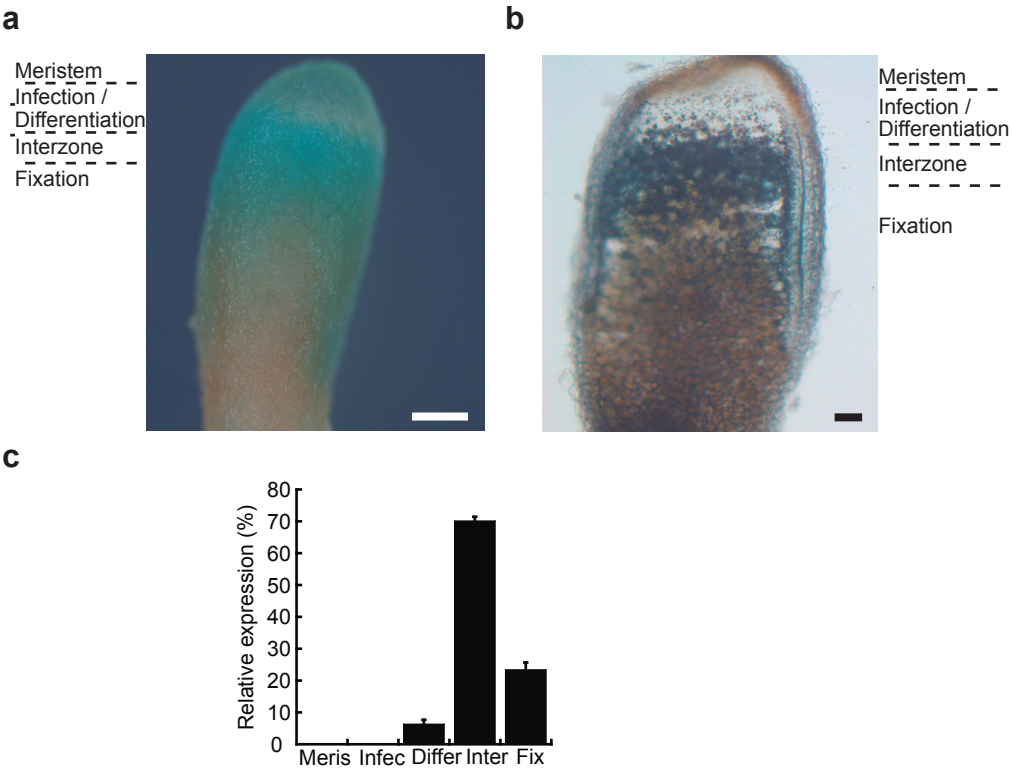

FIGURE 4

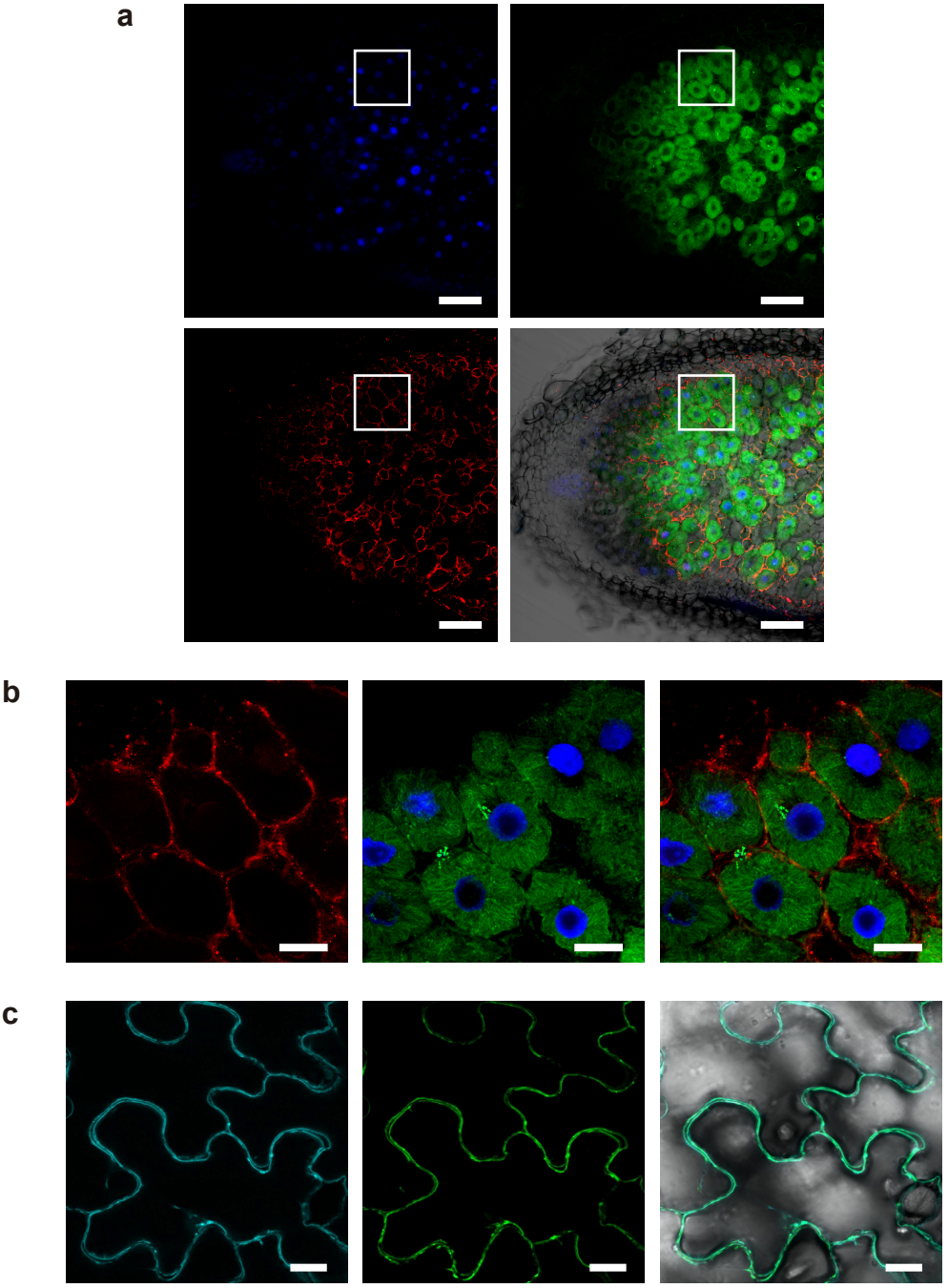

FIGURE 5

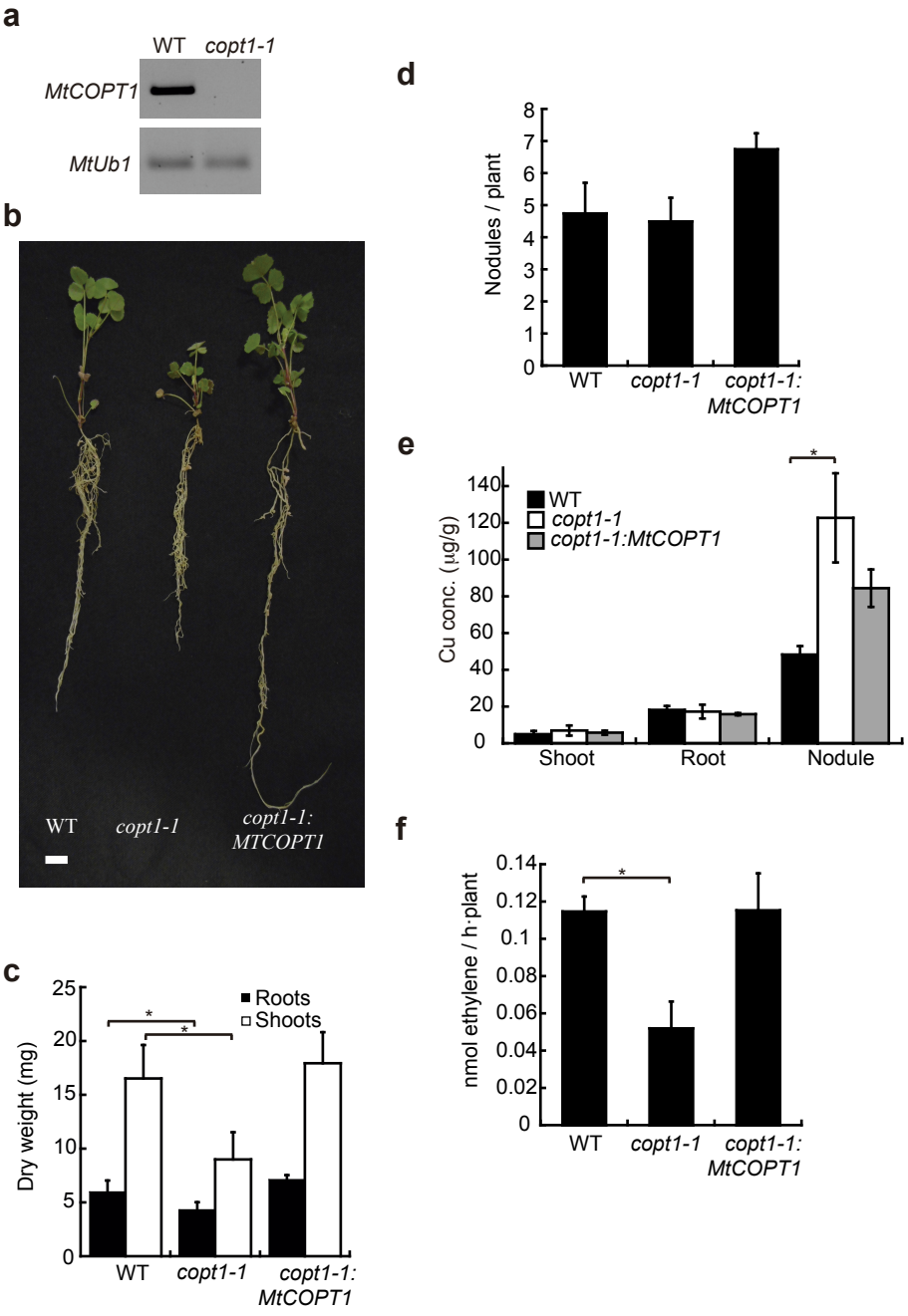

FIGURE 6

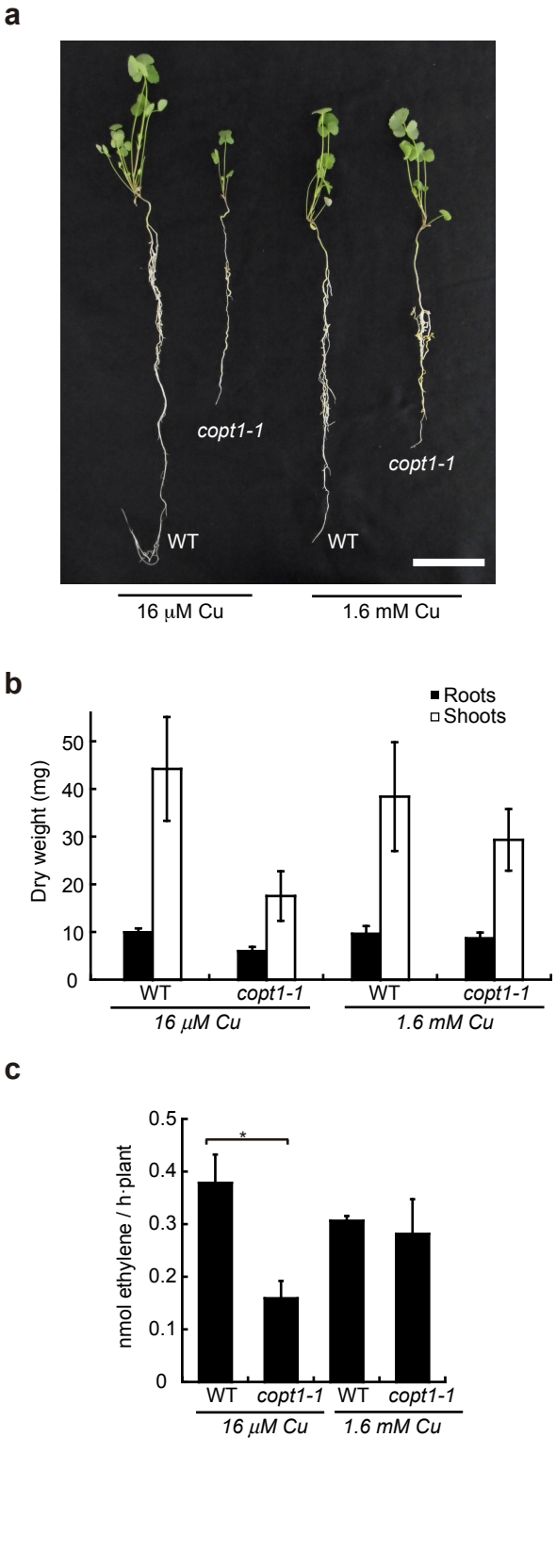

FIGURE 7

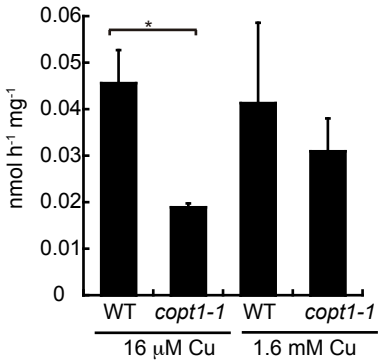

FIGURE 8